Modeling and parameter estimation for point-actuated continuous-facesheet deformable mirrors

Curtis Vogel,[1,*] Glenn Tyler,[2] Yang Lu,[3] Thomas Bifano,[4] Rodolphe Conan,[5] and Celia Blain[5]

[1]*Department of Mathematical Sciences, Montana State University, Bozeman, Montana 59717-2400, USA*
[2]*The Optical Sciences Company, 1341 South Sunkist Street, Anaheim, California 92806, USA*
[3]*Department of Mechanical Engineering, Boston University, Boston, Massachusetts 02215, USA*
[4]*Boston University Photonics Center, Boston University, Boston, Massachusetts, 02215, USA*
[5]*Adaptive Optics Laboratory, MECH, University of Victoria, Victoria, British Columbia V8W 3P6, Canada*
**Corresponding author: curtis.r.vogel@gmail.com*

Received January 13, 2010; revised June 23, 2010; accepted June 27, 2010;
posted June 29, 2010 (Doc. ID 122675); published July 26, 2010

We present a variant of the model introduced by Vogel and Yang [J. Opt. Soc. Am. A **23**, 1074 (2006)] for point-actuated deformable mirrors (DMs) with continuous facesheets, and we describe a robust efficient regularized-output least-squares computational scheme to estimate the parameters in the model, given noisy discrete observations of the DM response to known actuation. We demonstrate the effectiveness of this approach with experimental data obtained from a pair of DMs—a piezo-actuated prototype DM built by CILAS for the Thirty Meter Telescope Project and an electrostatically actuated commercial micro-electro-mechanical systems (MEMS) DM produced by Boston Micromachines Corporation. © 2010 Optical Society of America

OCIS codes: 010.1080, 230.4040.

1. INTRODUCTION

This work is based on the partial differential equation (PDE) model for point-actuated continuous-facesheet deformable mirrors (DMs) introduced by Vogel and Yang [1]. A key idea in [1] was the use of the thin plate equation [2], a fourth order PDE in two space variables, to model the effects of facesheet (plate) flexure. At steady state, flexural forces are balanced by forces due to the actuators attached to the facesheet. An additional idea introduced in [1] was to employ an algebraic equation for each of the actuators, relating the actuator voltage, actuator deflection, and force on the actuator due to the facesheet. In this paper we present refinements of this model to better account for the behavior of a pair of continuous-facesheet DMs—a 57-actuator piezo DM prototype [3] delivered by the CILAS Company for the Thirty Meter Telescope (TMT) Project and a commercially available 140-actuator electrostatic micro-electro-mechanical systems (MEMS) micromirror produced by the Boston Micromachines Company (BMC) [4]. We also introduce a robust efficient computational scheme to estimate the parameters in the model from interferometric measurements of the DM surface response to known actuation, and we demonstrate the effectiveness of this approach with data obtained from the CILAS and BMC mirrors.

This work is motivated by the need for control of DMs in ground-based astronomical adaptive optics (AO) where direct feedback is not available. An important application is multi-object AO [5,6], where multiple DMs must compensate for directionally dependent wavefront aberrations that have been computed using a tomographic reconstruction scheme. The pseudo-open-loop control concept in multi-conjugate AO [6,7], where DM deflections (assumed to be known) are used to modify closed-loop wavefront sensor measurements to compute a proxy for open-loop sensor measurements, will also benefit from accurate modeling of DM response to a known actuator input.

Similar MEMS DM modeling efforts have been carried out by Stewart *et al.* [4] at Boston University and by Morzinski *et al.* [8] from the Laboratory for Adaptive Optics at the University of Santa Cruz. We provide here a brief comparison with our modeling approach. All three approaches employ variants of the thin plate equation to model the DM facesheet. Stewart *et al.* [4] found it necessary to incorporate an additional second order term in their MEMS DM model to account for the effects of facesheet stretching. Our model to be presented in this paper also has a second order stretching term, but it is linear while Stewart's is nonlinear. The Morzinski model was based on the Green's function for the thin plate equation and has no such stretching term.

All three approaches use algebraic models for actuator effects. In [1] a "response surface" or a "look-up table," relating the voltage, actuator deflection, and force due to the facesheet acting on the actuator, was constructed by solving a separate actuator PDE model with varying voltage and facesheet force used as model inputs. Insufficient data were available to the authors for calibration, so only a qualitative comparison was made against the actual MEMS DM behavior. Morzinski *et al.* [8] and Stewart *et al.* [4] also employed actuator look-up tables, but theirs were constructed from actual measurements of MEMS DM deflection. It should be noted that facesheet forces on

the actuators cannot be measured directly; more will be said about this below.

Any approach to DM modeling will require model parameter selection. Certain parameters can be selected based on physical and material properties, e.g., the flexural rigidity of a thin plate is a known function of the plate thickness and the modulus of elasticity and the Poisson's ratio for the plate material [2]. Other parameters, e.g., the actuator spring "constant," may be impossible to measure directly and may depend in a complicated manner on the applied force, deflection, and applied voltage. In this paper we employ an output least-squares (OLS) [9] approach to parameter estimation. This means that we can express the model facesheet deflection (the "output") as a function of model parameters and voltages applied to the actuators. We vary the applied voltages and select model parameters which match, in a least-squares sense, the model deflection to the corresponding measured facesheet deflection.

The OLS approach is quite robust and can directly handle measurement error and sparse data. However, the implementation requires a high degree of mathematical and computational sophistication. In the work presented here, we rely on a finite element discretization of the PDE model, a sparse linear algebraic solver to compute DM deflection in terms of model parameters, and nonlinear optimization techniques to estimate these parameters.

Stewart *et al.* [4] took a significantly different approach to parameter estimation, employing what is known in the inverse problems community as the *equation error method* [10]. They numerically differentiated their measured data in a manner consistent with their facesheet PDE model in order to obtain (approximations to) the forces due to the facesheet at the actuator locations. They then fit actuator model parameters to data consisting of (approximate) actuator forces, measured actuator deflections, and known input voltages in order to construct their actuator lookup table. This approach is elegant in its simplicity, but the data must be of sufficiently high resolution to accurately compute fourth order partial derivative approximations, and care must be taken to filter out the noise.

This paper is organized as follows. In Section 2 we lay out our modeling assumptions, and we present the PDE that constitutes the DM model. In Section 3 we present the method of the OLS to estimate DM model parameters, and we detail the use of the adjoint method to increase robustness and reduce computational cost. In Section 4 we present experimental results obtained with the 57-actuator CILAS prototype DM and a 140-actuator MEMS mirror produced by Boston Micromachines Corporation. Section 5 presents the summary and concluding remarks.

2. DM MODEL

The physical assumptions underlying our mathematical model are as follows:

A1. The (temporal) dynamics of the DM facesheet are fast relative to the temporal changes in actuation. As a consequence, our equations are independent of time.

A2. The DM facesheet is a thin, elastic, and stretched linear plate. This allows us to use a variant of the two-dimensional (2-d) plate equation [2] to model the facesheet.

A3. Forces on the facesheet due to actuator loading are balanced by restoring force due to flexure and stretching of the facesheet.

A4. Each DM actuator applies a load to the facesheet over a relatively small area. This motivates our use of the Dirac delta "function" in our description of the actuator load.

A5. Actuator deflection depends linearly on the load induced by the facesheet and it depends linearly on the *actuation*. By actuation, we mean the square of the applied voltage in the case of electrostatically actuated MEMS DMs. For the CILAS DM analyzed in this paper, with lead zirconate titanate (PZT) actuators [3], the actuation is set equal to the applied voltage.

Our facesheet model takes the form

$$D_{\mathrm{fs}}\nabla^4 w - T\nabla^2 w + \sum_{i=1}^{n_a} p_i \delta(\mathbf{x}-\mathbf{x}_i) = 0, \tag{1}$$

where $w(\mathbf{x})$ denotes the deflection (out-of-the-neutral-plane displacement) of the facesheet at location $\mathbf{x}=(x,y)$ in the neutral plane, p_i denotes the load (force per unit area) due to the ith actuator at location $\mathbf{x}_i$, n_a denotes the number of actuators, $\delta(\ )$ denotes the Dirac delta, ∇^2 denotes the 2-d Laplacian operator, and

$$\nabla^4 w = (\nabla^2)^2 w = \frac{\partial^4 w}{\partial x^4} + 2\frac{\partial^4 w}{\partial x^2\,\partial y^2} + \frac{\partial^4 w}{\partial y^4} \tag{2}$$

is the 2-d biharmonic operator. The terms on the left-hand-side of the equal sign in model (1) represent, respectively, the loads due to flexure, stretching, and actuation; see Chapter 1 of [2] for the derivation and detailed discussion. The model parameters are the flexural rigidity D_{fs} and the tension T. We also impose free boundary conditions [2] at the edges of the facesheet. If assumption A4 does not hold, then the Dirac delta in Eq. (1) can be replaced with some (hopefully known) function which describes how the actuator load is distributed across the facesheet.

We employ a scalar model which is affine-linear in the DM deflection w for each of the actuators,

$$k(w(\mathbf{x}_i)-z_i) = A(p_i+\gamma a_i), \quad i=1,\ldots,n_a. \tag{3}$$

Here a_i denotes the *actuator command*; $w(\mathbf{x}_i)$ is the facesheet deflection at the ith actuator; and, as in Eq. (1), p_i is the load on the facesheet due to ith actuator. The left-hand-side of Eq. (3) can be interpreted as force due to spring-like behavior of the actuator, while the right-hand-side accounts for force due to the facesheet and electrostatic/piezo-electric force. The parameters in this model are the actuator *spring stiffness constant* k, the area of contact A between the actuator and the facesheet, the actuator gain coefficient γ, and the local offset z_i in the facesheet deflection.

As noted in assumption A5, for electrostatically actuated MEMS DMs, we take $a_i=V_i^2$, where V_i are the applied voltages. The offsets z_i account for surface varia-

tions in the unactuated DM that occur on length scales greater than the inter-actuator spacing. These may be due, for example, to MEMS foundry processes and mirror polishing. To accurately describe the CILAS DM, the offsets z_i are not needed (they are set to zero), and we take $a_i = V_i$.

If we solve for $p_i = (k/A)[w(\mathbf{x}_i) - z_i] - \gamma a_i$ in actuator (3) and substitute into the facesheet model (1), we obtain the reduced DM model,

$$\nabla^4 w - \beta_3 \nabla^2 w + \beta_2 \sum_{i=1}^{n_a} w(\mathbf{x}_i)\delta(\mathbf{x} - \mathbf{x}_i) = \beta_1 \sum_{i=1}^{n_a} a_i \delta(\mathbf{x} - \mathbf{x}_i) + \sum_{i=1}^{n_a} \beta_{0,i}\delta(\mathbf{x} - \mathbf{x}_i), \quad (4)$$

with parameters

$$\beta_3 = T/D_{\mathrm{fs}},$$

$$\beta_2 = k/AD_{\mathrm{fs}},$$

$$\beta_1 = \gamma/D_{\mathrm{fs}},$$

$$\beta_{0,i} = z_i k/AD_{\mathrm{fs}} = z_i \beta_2, \quad i = 1, \ldots, n_a.$$

Given parameter values, we solve the reduced model (4) numerically, using a Galerkin-finite element method with bicubic Hermite basis functions [11].

3. PARAMETER ESTIMATION

In order to estimate the parameters $\beta_{0,i}$ (with $i = 1, \ldots, n_a$), β_1, β_2, β_3 in the reduced model (4), we apply the method of the OLS [9]. We conduct a sequence of n_{exp} experiments with known actuator command vectors $\mathbf{a}_k$, and we measure the corresponding DM deflections with an interferometer on an $M \times N$ grid. This gives us a sequence of data vectors of length MN, which we denote by $w^{\mathrm{obs}}(\mathbf{a}_k)$, with $k = 1, \ldots, n_{\mathrm{exp}}$.

The Galerkin-finite element method that we apply to Eq. (4) yields solutions with a representation

$$w(x,y) = \sum_{\ell=1}^{n} w_\ell \psi_\ell(x,y),$$

where the basis functions ψ_ℓ are tensor products of piecewise cubic Hermite polynomials. w_ℓ are components of a vector $\mathbf{w} = \mathbf{w}(\beta; \mathbf{a}_k)$ that solves a linear system of the form

$$A(\beta_2, \beta_3)\mathbf{w} = \beta_1 F \mathbf{a}_k + \mathbf{b}(\beta_0). \quad (5)$$

In order to directly compare interferometer measurements of DM deflection with model predictions, we define the *observation operator* L, which maps Galerkin-finite element method solution vectors to the $M \times N$ interferometer measurement arrays, by

$$[L\mathbf{w}]_{ij} = \sum_{\ell=1}^{n} w_\ell \psi_\ell(x_i, y_j), \quad i = 1, \ldots, M, \quad j = 1, \ldots, N,$$

where the points (x_i, y_j) lie on the interferometer measurement grid.

We take our estimate for the parameter vector $\beta = (\beta_3, \beta_2, \beta_1, \beta_0)$, with $\beta_0 = (\beta_{0,1}, \ldots, \beta_{0,n_{\mathrm{act}}})$, to be the minimizer of the OLS cost functional

$$J_{\mathrm{OLS}}(\beta) = \frac{1}{2} \sum_{k=1}^{n_{\mathrm{exp}}} \| L\mathbf{w}(\beta, \mathbf{a}_k) - w^{\mathrm{obs}}(\mathbf{a}_k) \|^2 + \alpha \frac{1}{2} \beta_0^T R \beta_0. \quad (6)$$

The first term on the right-hand-side is a measure of data fidelity, while the second term is a regularization function, whose purpose is to impose stability by penalizing unreasonable estimates of the parameter vector β_0, which depends on the DM offsets z_i. In practice we take the matrix R to be the discrete 2-d Laplacian. α in Eq. (6) is a positive parameter which quantifies the trade-off between data fidelity and stability.

Note that the total number of parameters to be estimated is $n_{\mathrm{act}} + 3$. We employ an unconstrained minimization code, *fminunc*, from the MATLAB [12] optimization toolbox. In its default mode, *fminunc* numerically approximates the gradients of J_{OLS} using numerical centered differences. This requires $2(n_{\mathrm{act}} + 3)$ solutions of systems of the form (4) plus some additional overhead. By employing adjoint methods, we can dramatically reduce this cost and also eliminate possible numerical instabilities due to the difference approximation.

A. Adjoint Gradient Computations

For simplicity of the presentation, we first assume a single experiment. Then we can express the data-dependent portion of the OLS cost functional as

$$J(\beta) = \frac{1}{2} \langle \mathbf{r}(\beta), \mathbf{r}(\beta) \rangle, \quad (7)$$

where $\langle\ ,\ \rangle$ represents Euclidean inner product and the fit-to-data residual

$$\mathbf{r}(\beta) = L\mathbf{w}(\beta, \mathbf{a}) - \mathbf{w}^{\mathrm{obs}} = LA(\beta_2, \beta_3)^{-1}(\beta_1 F \mathbf{a} + \mathbf{b}(\beta_0)) - \mathbf{w}^{\mathrm{obs}}. \quad (8)$$

Because it appears as a simple multiplicative factor in Eqs. (4) and (5), we will first examine the gradient component associated with β_1,

$$\frac{\partial J}{\partial \beta_1} = \left\langle \frac{\partial \mathbf{r}}{\partial \beta_1}, \mathbf{r} \right\rangle = \langle LA^{-1}F\mathbf{a}, \mathbf{r} \rangle = \langle F\mathbf{a}, \mathbf{u} \rangle, \quad (9)$$

where

$$\mathbf{u} = A^{-1}L^T\mathbf{r}. \quad (10)$$

The last equality (9) follows by taking adjoints. Note that as a consequence of the structure of the PDE (4), the free boundary conditions, and the Galerkin discretization, A is a symmetric matrix, so $(A^{-1})^T = A^{-1}$.

From the last term on the right-hand-side of Eq. (4), we can express

$$\mathbf{b}(\beta_0) = \sum_{i=1}^{n_{\mathrm{act}}} \beta_{0,i} \mathbf{b}_i,$$

where Galerkin discretization yields vector components

$$[\mathbf{b}_i]_j = \int\int \delta(\mathbf{x}-\mathbf{x}_i)\psi_j(\mathbf{x})\mathrm{d}\mathbf{x} = \psi_j(\mathbf{x}_i).$$

Following the derivation of Eq. (9), for $i=1,\ldots,n_{\mathrm{act}}$,

$$\frac{\partial J}{\partial \beta_{0,i}} = \left\langle \frac{\partial \mathbf{r}}{\partial \beta_{0,i}}, \mathbf{r} \right\rangle = \langle \mathbf{b}_i, \mathbf{u} \rangle. \tag{11}$$

To obtain components of the gradient with respect to β_2 and β_3, we apply the product rule to the identity $A^{-1}A=I$ to obtain

$$\frac{\partial A^{-1}}{\partial \beta_i} = -A^{-1}\frac{\partial A}{\partial \beta_i}A^{-1}, \quad i=2,3.$$

Then for $i=2,3$,

$$\frac{\partial J_{\mathrm{OLS}}}{\partial \beta_i} = -\left\langle \frac{\partial A}{\partial \beta_i}\mathbf{w}, \mathbf{u} \right\rangle. \tag{12}$$

With multiple experiments, we can express the gradient of J_{OLS} as

$$\mathbf{g} = \sum_{k=1}^{n_{\mathrm{exp}}} \mathbf{g}_k + \alpha \mathbf{g}_{\mathrm{reg}}, \tag{13}$$

where the components of $\mathbf{g}_k$ are computed as in Eqs. (9)–(12), with $\mathbf{a}$ replaced with $\mathbf{a}_k$. For each k, this requires the solution of only two (discrete) sparse linear systems involving the matrix $A=A(\beta_1,\beta_2)$: Eq. (5) to get the "state vector" $\mathbf{w}_k$ and Eq. (10) to obtain the "adjoint vector" or "costate vector" $\mathbf{u}_k$. There is some relatively minor additional computational overhead involving, for example, dot products. The components of $\mathbf{g}_{\mathrm{reg}}$ in Eq. (13) are obtained by taking partial derivatives of the regularization term,

$$\frac{\partial}{\partial \beta_{0,i}}\left(\frac{1}{2}\beta_0 R \beta_0\right) = [R\beta_0]_i, \quad i=1,\ldots,n_{\mathrm{act}},$$

and requiring only a single sparse matrix multiply involving the discrete 2-d Laplacian matrix R.

In summary, when this adjoint approach is implemented, the computational cost of a gradient evaluation is dominated by $2n_{\mathrm{exp}}$ sparse linear system solutions involving the matrix A. In contrast, the centered finite difference approach requires $2n_{\mathrm{exp}}(n_{\mathrm{act}}+3)$ such linear system solutions—roughly a factor of n_{act} greater expense.

4. EXPERIMENTAL RESULTS

A. CILAS DM Results

We first consider the prototype DM [3] built by CILAS for the TMT Project. This DM was rigorously tested by TMT partners with the Adaptive Optics Laboratory at the University of Victoria, Canada [13]. Results presented here make use of some of their evaluation data.

This DM has 57 controllable actuators evenly located on a 9×9 grid inside a circular pupil. There are additional two rows of actuators on the outside that cannot be controlled. The DM inter-actuator spacing and coupling are 5 mm and 20%, respectively. A single actuator stroke is 10 μm and the inter-actuator stroke is 1.9 μm. Actuator hysteresis is around 5%. The DM facesheet is made of a thin glass plate cemented on a low expansion metallic material that links the actuators to the glass plate.

The facesheet of the CILAS DM is relatively thick compared to actuator-induced deflections. It was also quite stiff, so stretching effects are minimal. For this reason, we were able to omit the Laplacian (stretching) term in the facesheet model (1). In addition, the actuators were composed of PZT, which exhibits a linear voltage-to-displacement response. Also, the unactuated CILAS DM facesheet is very flat and the actuators are quite uniform. This enables us to replace the actuator model (3) with

$$kw(\mathbf{x}_i) = A(p_i + \gamma a_i), \quad a_i = V_i. \tag{14}$$

The reduced model (4) then simplifies to

$$\nabla^4 w + \beta_2 \sum_{i=1}^{n_a} w(\mathbf{x}_i)\delta(\mathbf{x}-\mathbf{x}_i) = \beta_1 \sum_{i=1}^{n_a} a_i \delta(\mathbf{x}-\mathbf{x}_i), \tag{15}$$

with only two parameters,

$$\beta_2 = k/AD_{\mathrm{fs}}, \quad \beta_1 = \gamma/D_{\mathrm{fs}}. \tag{16}$$

A critical first stage in the parameter estimation process is to accurately determine the locations of the actuators in the neutral plane of the facesheet. This was done by poking (i.e., applying nonzero voltage to) each individual actuator while keeping all the remaining actuators at zero voltage, measuring the facesheet deflection interferometrically, and then finding the neutral-plane coordinates of the points of peak deflection.

Once the actuator coordinates are known, they can be mapped to a 2-d finite element grid, and simulations can be carried out using the parameter-dependent model (15). One can accurately determine the pair of parameters in Eq. (16) using the techniques of Section 3 from a single "parameter estimation" experiment, shown in Fig. 1. In this experiment only the center actuator was poked, i.e., nonzero voltage was applied to it, while zero voltage was applied to all the remaining actuators.

Four separate subplots are used to present the results of this parameter estimation experiment. The upper right subplot shows the measured DM deflection, the upper left subplot shows simulated DM deflection, the lower left subplot shows the difference between simulated and measured deflections, and the lower right subplot shows

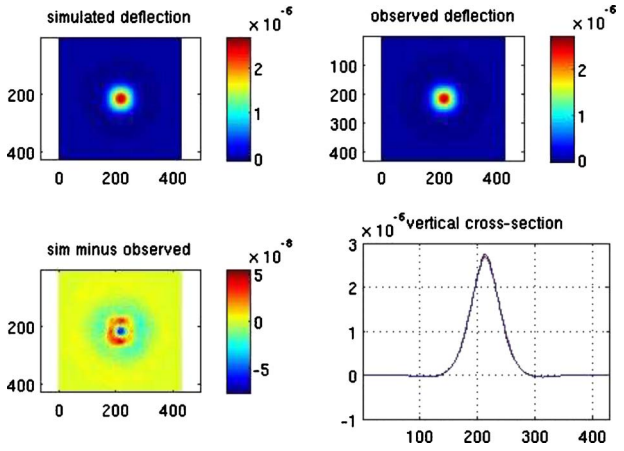

Fig. 1. (Color online) Results of the parameter estimation experiment for the CILAS DM.

cross-sections of the deflections through the poked actuator. The solid blue curve represents the measured cross-section while the dashed red curve corresponds to the simulated cross-section.

In order to determine the effectiveness of the modeling/parameter estimation scheme, we conducted a "validation experiment," shown in Fig. 2. In this case, we took the parameters generated from the previously described (single poke) estimation experiment and simulated the DM response to a 3×3 block of poked actuators, again using Eq. (15), and compared it to measured data. The four subplots in Fig. 2 are analogous to the subplots shown in Fig. 1; the cross-sections in the lower right are through the center of the 3×3 actuator block. The modeling error (simulated minus observed DM deflection) for the parameter estimation experiment was 4.6 nm root mean squared (RMS), while the RMS modeling error for the validation experiment was 90 nm.

B. Boston Micromachines MEMS DM Results

The MEMS DM used in this experiment is a commercial 140-actuator device, the Multi-DM produced by Boston Micromachines Corporation. The DM facesheet is a polycrystalline silicon block measuring approximately 3 μm in thickness and 6 mm$\times$6 mm in span. The electrostatic actuators lay on a regular 16×16 grid and are attached to the facesheet via rigid posts; see [4] for a detailed description. The interior 12×12 array, absent its corners, provides the subset of 140 actuators that are controllable. Other actuators form identical mechanical constraints, but are not addressable.

There are significant differences between this MEMS DM and the CILAS DM. The MEMS inter-actuator spacing of 400 μm is more than a factor of 10 smaller than for the CILAS DM. In addition, the MEMS facesheet is much thinner and less stiff than the CILAS facesheet, so facesheet stretching may be much more significant. Moreover, the unactuated CILAS DM has a very flat surface, while the unactuated MEMS DM facesheet has a significant bulge or "bow" across its center. Finally, hysteresis is negligible for the MEMS DM but not for the CILAS DM.

After obtaining the actuator locations for this DM, we conducted a pair of *differential deflection experiments* in order to test the validity of some of our modeling assumptions. We first applied a 141 V "bias" to all 140 controllable actuators and measured the resulting bias deflection. We then applied a sequence of ten separate voltages or "pokes" to the actuator at location (6,6) in the 12×12 grid of controllable actuators, while keeping all the other actuators at the bias voltage, and we measured the resulting facesheet deflections. The voltages in the poke sequence ranged from 0 to 200 V and were equally spaced in V^2. The differential deflection is equal to the poke deflection minus the bias deflection. The *peak differential deflection* is the differential deflection of largest magnitude, which occurs at the poked actuator.

We then repeated the process, except with the sequence of poke voltages applied to the 3×3 block of actuators centered at actuator (6,6). For both experiments, we computed a best least-squares fit of the peak differential deflection data d_i to the one-parameter linear model

$$d_i = \tilde{\gamma}(V_i^2 - V_{\text{bias}}^2), \quad i = 1, \ldots, 10. \tag{17}$$

The results are presented in Fig. 3. If the linear facesheet model (1) is valid (equivalently, if modeling assumption A2 holds), then these results suggest that the DM model (3) is valid (equivalently, assumption A5 holds) for voltages that are near the bias voltage. The deviation from linearity seen here for 3×3 block pokes when voltages are not close to bias is consistent with the results reported by Blain *et al.* [14].

The MEMS DM model (4) is much more complex than model (15) used for the CILAS DM, having $n_{\text{act}}+3$ parameters (=143, for the 140-actuator MEMS device) rather than just two parameters. For this reason, we found it necessary to conduct five separate estimation experiments, rather than a single experiment. A sixth validation experiment was carried out for evaluation purposes. The actuator poke patterns for each of these experiments are described below.

Experiment 1. 141 V bias applied to all actuators (no pokes).

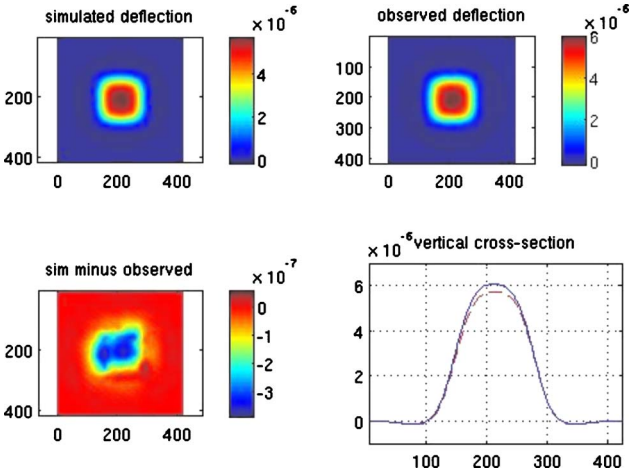

Fig. 2. (Color online) Results of the validation experiment for the CILAS DM.

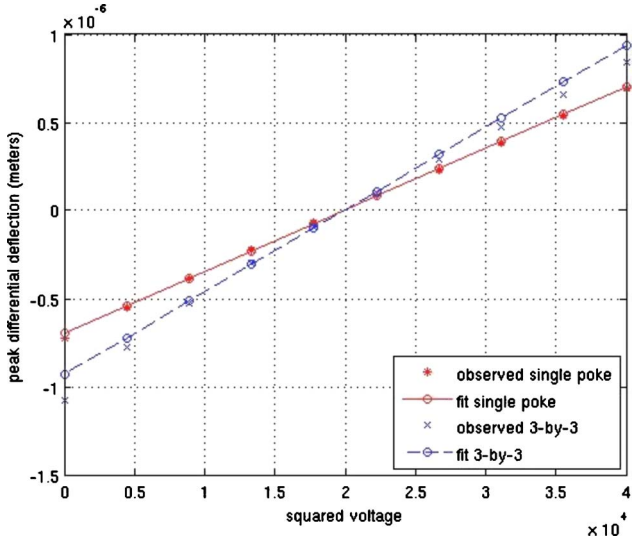

Fig. 3. (Color online) Peak differential deflections versus squared voltage for the Boston Micromachines MEMS DM.

Experiment 2. 67 V applied to actuator (6,6); 141 V bias applied to remaining actuators.

Experiment 3. 189 V applied to actuator (6,6); 141 V bias applied to remaining actuators.

Experiment 4. 115 V applied to a 3×3 block of actuators centered at (6,6); 141 V bias applied to remaining actuators.

Experiment 5. 163 V applied to a 3×3 block of actuators centered at (6,6); 141 V bias applied to remaining actuators.

Validation experiment. 115 V applied to a 2×2 block of actuators with indices (6,6), (6,7), (7,6), (7,7); 141 V bias applied to remaining actuators.

In an attempt to stay within the linear range of the DMs, we applied voltages that were closer to bias for the 2×2 and 3×3 poke experiments than we did for the single poke experiments; see Fig. 3. Results from all six MEMS DM experiments appear in Fig. 4. The four subplots for each experiment are analogous to those shown previously for the CILAS DM experiments. For all experiments, including the validation experiment, the RMS error between the simulated and observed deflections was less than 10 nm.

5. SUMMARY AND CONCLUSIONS

In this paper we presented a variant of the model for DMs with continuous facesheets and point actuation which was introduced by Vogel and Yang [1], and we described a regularized output least-squares (OLS) scheme to estimate the model parameters. To improve robustness and reduce computational cost, an adjoint approach was implemented to compute the gradients of the OLS cost function. The effectiveness of the modeling approach and the parameter estimation scheme was demonstrated for two DMs. The first was a 57-actuator prototype DM built by CILAS for the Thirty Meter Telescope (TMT) Project, and the second was a 140-actuator MEMS DM produced by Boston Micromachines Corporation. The former DM has piezo-ceramic actuators and a relatively thick stiff facesheet, while the latter has electrostatic actuators and a relatively thin flexible facesheet.

The reduced model, obtained by combining a facesheet model with an actuator model, is a fourth order linear time-independent partial differential equation (PDE) in two space variables for the DM deflection. This equation consists of a biharmonic term, a Laplacian term, and a superposition of Dirac delta damping terms on the left-hand-side, along with a right-hand-side that combines actuation and offset terms, each involving Dirac deltas at the actuator locations. This model has n_a+3 "reduced" parameters, where n_a is the number of DM actuators, which are combinations of physical parameters that include the facesheet flexural rigidity and tension, the actuator spring constant and area of contact with the facesheet, actuation (voltage or squared voltage, depending on the type of actuator) gain, and the actuator offsets. These offsets are necessary to accommodate large low spatial frequency deflections in continuous-facesheet MEMS DMs that arise from MEMS foundry and polishing processes. The CILAS DM required only two reduced parameters, which depend on the DM flexural rigidity, the actuator spring constant, and the actuation gain.

The regularized OLS method was applied with measured deflection data from both DMs, obtained interferometrically, to estimate the reduced model parameters. For the CILAS DM, only a single experiment, in which one actuator was poked and all the others were held at a bias voltage, was required to estimate the two reduced model parameters. To obtain the $n_a+3=143$ reduced parameters for the MEMS DM, we used data from five separate experiments. These experiments involved holding all actuators at a constant 141 V bias voltage, poking a single actuator near the center of the mirror with a pair of distinct voltages, and applying a pair of different voltages to a 3×3 block of actuators.

After estimating the parameters, we conducted an additional validation experiment for each DM, in which we applied poke patterns that were different from those used in the estimation experiments. With the new poke patterns, we measured the resulting DM deflections and compared them with model predictions generated with previously estimated model parameters.

For the CILAS DM, we obtained excellent agreement between the modeled DM deflection and the measured deflection in the estimation experiment. The modeling error was only 4.6 nm RMS, compared with a nearly 3 μm peak deflection. The modeling error for the validation experiment was significantly larger—90 nm RMS, compared to a peak deflection of about 6 μm. For the MEMS DM, the agreement between the model and the observations was quite good for each of the five estimation experiments as well as for the validation experiment. In all cases, the MEMS modeling error never exceeded 10.0 nm; for the validation experiment the error was 9.5 nm, compared to a peak-to-valley difference in deflection across the DM of slightly more than 500 nm.

The relatively large modeling error for the CILAS DM observed in the validation experiment is probably due to (nonlinear) hysteresis effects from the piezo-ceramic materials used in the actuators. Tests conducted at the University of Victoria Laboratory for Adaptive Optics indicated that the hysteresis never exceeded 5% of the peak-to-valley deflection range of the DM. The modeling discrepancy observed here is well within that range. The analysis in [7], in which the effects of sensor and actuator misalignment were considered, suggests that a linear DM model like the one used here may prove beneficial for pseudo-open-loop control for the TMT.

It should be noted that the MEMS DM modeling effort is working in progress. In particular, various nonlinear effects and their interactions are not well understood, and no attempt was made to model them in this paper. The relatively small modeling errors that were reported here are a consequence of the fact that we applied poke patterns and voltages that kept the DM deflections within the range of the linear model. Had we generated much larger deflections, results reported in [14] indicate that we would almost certainly have observed significantly larger modeling errors.

It is well-known that (MEMS) electrostatic actuator nonlinearities arise from electromechanical effects that occur when the actuator deflection becomes comparable to

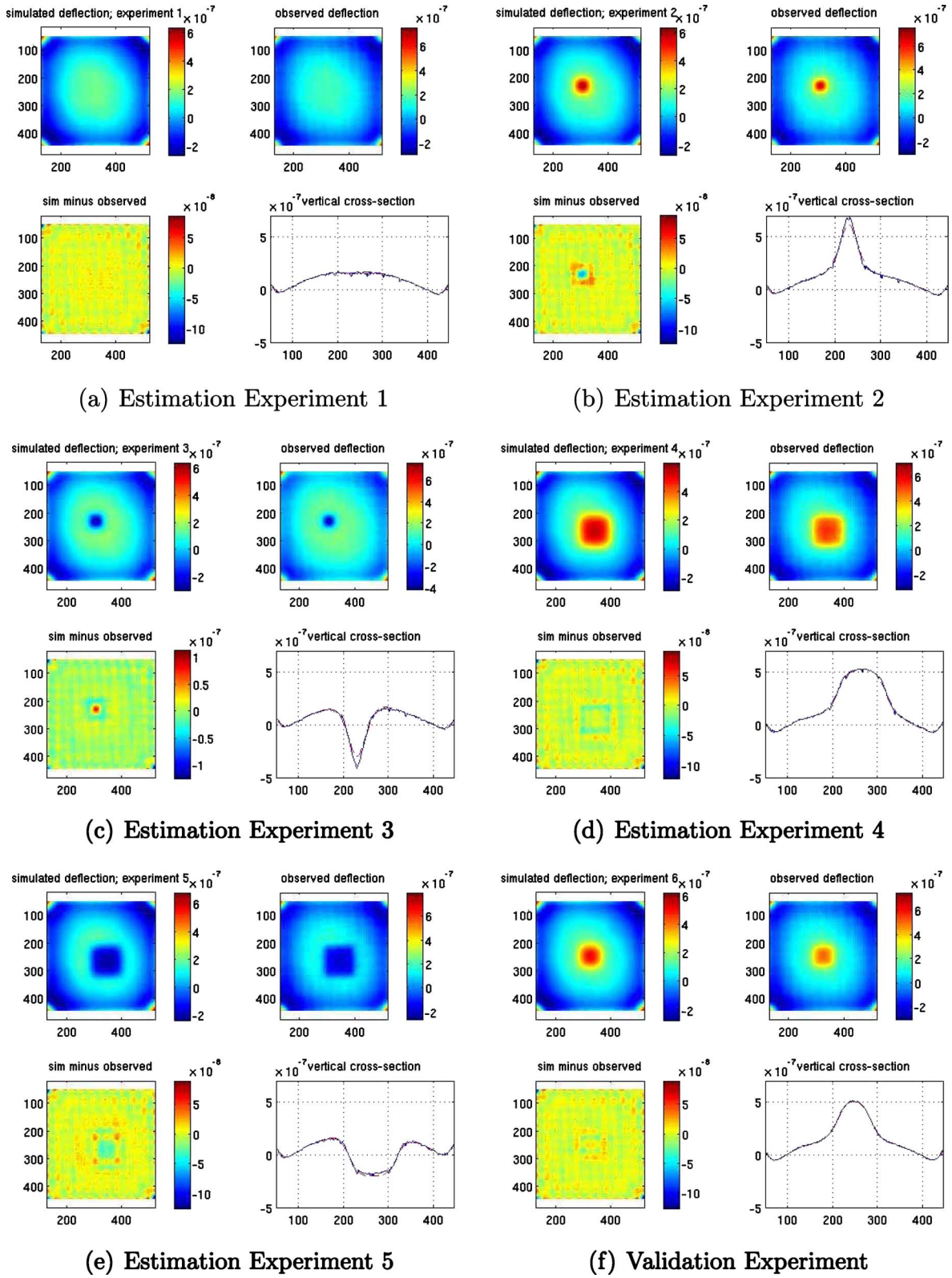

Fig. 4. (Color online) Results for the 140-actuator Boston Micromachines MEMS DM.

the gap size. It is also likely that large deflections will induce nonlinear plate behavior in the actuator plates. The latter phenomenon has been incorporated into many DM models (see, for example, [1,4]), while the former has been little studied. The modeling approach in [1] provides a computational framework with which to handle the latter nonlinearity. What is needed now are experiments and analyses with which to determine the exact nature of this nonlinearity and its interaction with the electromechanical nonlinearity. A mathematical model that accounts for

the nonlinear plate behavior of the DM facesheet has been incorporated in the work of Stewart *et al.* [4]. What is not known at this time is the significance of the facesheet nonlinearity relative to the actuator nonlinearities.

ACKNOWLEDGMENTS

Work at Boston University was supported by the National Science Foundation (NSF) Science and Technology Center for Adaptive Optics, managed by the University of California at Santa Cruz under cooperative agreement No. AST9876783. T. Bifano acknowledges a financial interest in Boston Micromachines Corporation. Support for G. Tyler came from the NSF Small Business Innovative Research Program Grant Number 0912623, awarded to the Optical Sciences Company (tOSC). C. Vogel was supported by a grant from tOSC to the Montana State University.

REFERENCES

1. C. R. Vogel and Q. Yang, "Modeling, simulation, and open-loop control of a continuous facesheet MEMS deformable mirror," J. Opt. Soc. Am. A **23**, 1074–1081 (2006).
2. S. Timoshenko and S. Woinowsky-Krieger, *Theory of Plates and Shells* (McGraw-Hill, 1959).
3. J.-C. Sinquin, J.-M. Luron, and C. Guillemard, "Deformable mirror technologies for astronomy at CILAS," Proc. SPIE **7015**, 7015–7023 (2008).
4. J. B. Stewart, A. Doiuf, Y. Zhou, and T. G. Bifano, "Open-loop control of a MEMS deformable mirror for large-amplitude wavefront control," J. Opt. Soc. Am. A **24**, 3827–3833 (2007).
5. F. Assémat, E. Gendron, and F. Hammer, "The FALCON concept: multi-object adaptive optics and atmospheric tomography for integral field spectroscopy," Mon. Not. R. Astron. Soc. **376**, 287–312 (2008).
6. B. L. Ellerbroek and C. R. Vogel, "Topical review: Inverse problems in atmospheric adaptive optics," Inverse Probl. **25**, 063001 (2009).
7. L. Gilles, "Closed-loop stability and performance analysis of least-squares and minimum-variance control algorithms for multi-conjugate adaptive optics," Appl. Opt. **44**, 993–1002 (2005).
8. K. M. Morzinski, K. B. W. Harpse, D. T. Gavel, and S. M. Ammons, "The open-loop control of MEMS: Modeling and experimental results," Proc. SPIE **6467**, 64670G (2007).
9. C. R. Vogel, *Computational Methods for Inverse Problems* (SIAM, 2002).
10. H. T. Banks and K. Kunisch, *Estimation Techniques for Distributed Parameter Systems* (Birkhuser, 1989).
11. C. R. Vogel and J. J. Heys, "Fast multigrid solution of biharmonic operator equations," preprint, Department of Mathematical Sciences, Montana State University, 2009.
12. MATLAB, The Mathworks, Natick, Mass., USA.
13. C. Blain, R. Conan, C. Bradley, O. Keskin, P. Hampton, and A. Hilton, "Magnetic ALPAO and piezo-stack CILAS deformable mirrors characterization," in *Adaptive Optics: Analysis and Methods/Computational Optical Sensing and Imaging/Information Photonics/Signal Recovery and Synthesis*, Topical Meetings on CD-ROM, OSA Technical Digest (CD) (Optical Society of America, 2007), paper ATuC6.
14. C. Blain, R. Conan, C. Bradley, O. Guyon, and C. R. Vogel, "Characterization of the influence function non-additivities for a 1024-actuator MEMS deformable mirror," in *Proceedings of First AO4ELT Conference—Adaptive Optics for Extremely Large Telescopes*, Y. Clenet, J.-M. Conan, T. Fusco, and G. Rousset, eds. (EDP Sciences, 2010), 06009.